Emission and Fluorescence Spectroscopy To Examine Shock-Induced Decomposition in Nitromethane

Yuri A. Gruzdkov* and Yogendra M. Gupta†

Institute for Shock Physics and Department of Physics, Washington State University, Pullman, Washington 99164-2816

Received: March 23, 1998; In Final Form: June 16, 1998

Time-resolved emission spectra were obtained from neat and ethylenediamine-sensitized nitromethane shocked to 12−17 GPa peak pressures using step wave loading. Broadband emission identified as chemiluminescence from nitrogen dioxide was observed due to reactions in both neat and amine-sensitized nitromethane. When laser light at 514 nm was present, fluorescence in addition to chemiluminescence was observed in shocked nitromethane−ethylenediamine mixtures; no such fluorescence was found in neat nitromethane. The fluorescing species are assigned to an intermediate formed in the first stage of decomposition in nitromethane−ethylenediamine mixtures. The same intermediate was detected previously using time-resolved optical absorption spectroscopy (*J. Phys. Chem. A* **1998**, *102*, 2322) and was inferred to be a radical anion of nitromethane, $CH_3NO_2^{\bullet-}$. This interpretation is consistent with the fluorescence data reported here. Laser irradiation (∼10 MW/cm^2 at 514 nm) during shock loading resulted in more intense chemiluminescence in both neat nitromethane and nitromethane−ethylenediamine mixtures. However, the effect was qualitatively different in the two cases, and the difference is attributed to different decomposition mechanisms operative initially in neat and sensitized nitromethane.

I. Introduction

Time-resolved optical spectroscopic techniques are being used increasingly to probe molecular processes governing shock-induced decomposition of energetic materials.[1] They have the advantage of being in situ microscopic probes that complement time-resolved continuum measurements. Hence, scientific issues relevant to the development of new energetic materials, shock sensitivity, and safety of high explosives can be addressed at a fundamental level.

Recently, time-resolved UV−vis optical absorption[2−5] and Raman[6−9] spectroscopy experiments have been undertaken in our laboratory on shocked nitromethane (NM), a prototypical energetic material. NM was chosen for a number of reasons: it is a liquid, and, therefore, the complexities associated with solid materials can be avoided; its chemical structure is relatively simple; and it has the advantage of variable sensitivity in the presence of amines.[10−14] Furthermore, NM is a very well-studied material; good reviews of earlier work on NM may be seen in refs 4 and 14, and short summaries are given in refs 3 and 15. Thus, information can be drawn from a large body of scientific literature which includes spectroscopic data at ambient pressure,[14] static high-pressure data,[16] and continuum data under shock loading.[17,18]

In neat NM subjected to stepwise shock loading to 14 GPa, no evidence for chemical reaction was observed within the 1 μs duration.[2,4−6,8] However, UV−vis absorption measurements on NM−amine mixtures subjected to 11 GPa stepwise loading showed irreversible changes in the spectra, ascribed to a chemical reaction onset; the pressure threshold for the reaction onset has not been established.[2,3] The changes consisted of a red shift of an electronic absorption band and the development of a new absorption band at 525 nm. Neat NM, when shocked to around 17 GPa, also reacted.[5] However, the changes in the neat NM spectra were quite different from those in amine-sensitized NM.[3] The former consisted mainly of a broadband loss of transmission after a short induction period.[3−5] This indicated that the initial stages of the reaction were likely different in neat and sensitized NM.

Raman measurements, however, revealed some similarities between neat and amine-sensitized NM after the reaction onset.[6,9] Particularly, quite intense light emission seen as a rapidly rising background was observed for both neat and sensitized NM. The origin of this emission was assigned tentatively to the luminescence of an unspecified reaction product.[6,9] Further clarification of this phenomenon from Raman measurements was intrinsically difficult owing to the narrow spectral coverage (500−3500 cm^{-1}, corresponding to the 528−627 nm range, with the 514.5 nm excitation wavelength).

In this work, we investigated the nature and origin of light emission in reacting NM and NM−ethylenediamine (EDA) mixtures. The experiments were designed to explore the possibility of using this emission to detect and identify chemical changes to the sample. Additionally, we addressed the issue of how the reaction is perturbed by the presence of laser excitation. The latter is important in determining the feasibility of Raman measurements in shocked reacting systems. The remainder of this paper is organized as follows: In the next section we describe briefly the experimental methods used in this work. Section III presents the experimental results. In section IV, we discuss the origin of emission and effects of

* To whom correspondence should be addressed. E-mail: gruzdkov@mail.wsu.edu.
† E-mail: ymgupta@wsu.edu.

10.1021/jp981588n CCC: $15.00
Published on Web 10/01/1998

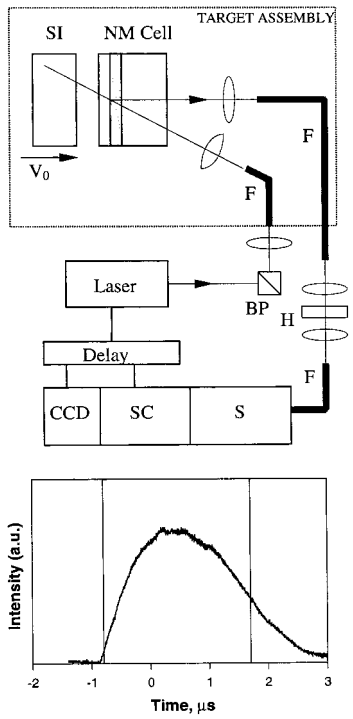

Figure 1. Schematic diagram of the experimental configuration. Shock waves are launched by impact between a sapphire impactor, SI, and the front window of the sample cell. Sample thickness (shaded area), typically 0.25 mm, is exaggerated in the drawing. For fluorescence measurements, a laser pulse excites the sample. The output of the laser is filtered by a band-pass filter, BP, and directed onto the sample through an optical fiber, F, at 45° incident angle. Light emitted from the shocked sample is collected into another optical fiber and delivered to the detection system consisting of a spectrometer, S, streak camera, SC, and CCD detector. A holographic notch filter, H, inserted into the delivery fiber line rejects the elastically scattered laser light. The laser, streak camera, and CCD detector are all synchronized with the arrival of the shock wave through appropriate time delays. The bottom graph depicts a typical laser pulse and its timing relative to the streak camera record (vertical lines) and shock wave (at 0 μs, shock enters the sample). For emission measurements, the laser is not fired and the holographic filter is removed.

laser interaction with the shocked material. The main findings are summarized in section V.

II. Experimental Method

A. Materials. All samples used in this work consisted of neat NM or NM−EDA mixtures (18.8 mM EDA concentration). Spectrophotometric grade NM of 99+% purity and ethylenediamine 99+ or 99.5+% were obtained from Aldrich Chemical Co. The chemicals were used as received except for EDA 99+% which was redistilled in the laboratory before use (experiments E7−E9). The NM−EDA mixtures were prepared in air 2−5 h before each experiment.

B. Overall Configuration. The experimental configuration used in this work was very similar to that used previously.[6,8,9] Therefore, except for new features, only a brief description of these experiments is presented. Details can be found elsewhere.[4]

Figure 1 shows a schematic diagram of the experimental configuration. Shock waves were generated by impact between a sapphire impactor, mounted on a projectile, and the front window of the sample cell. The projectile could be accelerated to any velocity up to 1.2 km/s using a single stage gas gun.[19] After traversing the front window, the shock wave reverberates between the cell windows, bringing the NM sample to the final pressure and temperature via a stepwise loading process. Final pressure is maintained in the sample until release waves arrive from the edges of the windows. Because the data are obtained only from the central 1 mm, the sample is in a state of uniaxial strain for over 1 μs.

The NM cell, shown in Figure 1, was identical to that described previously.[6,8] Either sapphire or LiF front windows and sapphire back windows were used (see Table1). As discussed earlier,[4−6] the use of the LiF front window causes the liquid to reach the final pressure in fewer reverberations, resulting in a higher temperature. To further increase the final temperature, we heated the sample prior to experiments E2−E4 with a heater coil inserted into the brass cell body.[4]

Pressure and temperature histories for the sample in each experiment were calculated using the SHOCKUP program.[20] The calculations used a material model describing the shock response of sapphire[21] and LiF[22] and the equation of state for NM developed in our laboratory.[4,7] Because the impact velocity and the shock response of the impactor and cell windows are well-known, the calculated final pressures should be accurate to within 1−2%. Our recent temperature measurements in shocked neat NM,[7] using Raman scattering, showed that the calculated temperatures are accurate to within 8−10%.

Light emitted from the shocked sample is collected by a lens assembly positioned along the normal to the cell back window. It is then directed into an optical fiber and delivered to the detection system[6,8] consisting of a spectrometer (Spex 500M), streak camera (Imacon 790, Hadland), and CCD detector (PI CCD, 1024 × 1024 back-illuminated chip). For fluorescence measurements, light from a pulsed dye laser (Cynosure SLL-5000, 514.5 nm; 3.5 μs pulse duration) is directed through another optical fiber onto the sample at 45° incident angle. The elastically scattered light is then rejected by a filter stage inserted into the collection fiber line. Using a trigger pin, the streak camera and the laser are synchronized through appropriate time delays with the arrival of the shock wave at the liquid sample.

The spectral response of the entire system (collection, dispersion, and detection components combined) was obtained using a National Institute of Standards and Technology (NIST) calibrated quartz−iodine lamp (GE type 6.6 A/T4Q/ILC-200 W). The true relative intensity spectrum of the source and the measured spectrum were fitted with sixth order polynomials. The correction function was obtained by taking the ratio of these polynomials. Using this function, the intensities were corrected in all the experimentally measured spectra. Only the corrected spectra were used in the analysis.

III. Results

Experimental details pertinent to the time-resolved emission and fluorescence experiments are summarized in Table 1. A total of nine experiments is presented: four experiments on neat NM and five on NM−EDA mixtures.

A. Neat Nitromethane. As mentioned earlier, the UV−vis absorption and Raman spectroscopy data provided no evidence for chemical reaction in neat NM at pressures below 14 GPa.[2,5] In agreement with these findings, no emission was observed in experiment E1. Therefore, to observe reaction within 1 μs, we performed experiment E2 at a peak pressure of 16.7 GPa.

Figure 2 shows a three-dimensional plot of experiment E2; a bright flash of emission occurred at ca. 650 ns after the shock wave entered NM. A representative spectrum of this emission is shown in Figure 3. The spectrum changes only slightly in time, leaving characteristic features nearly constant throughout

TABLE 1: List of Experiments

expt no.	sample	laser intens (mJ/pulse)	front window	cell thickness (μm)	initial temp (K)	projectile velocity (km/s)	calcd peak pressure[a] (GPa)	calcd peak temp (K)	spectral coverage (nm)
E1 (95-015)	NM	140	sapphire	274	ambient	0.611	13.9	765	510−620
E2 (96-019)	NM	0	LiF	229	323	0.909	16.7	978	380−750
E3 (95-025)	NM	1	LiF	272	323	0.929	17.1	990	460−570
E4 (95-024)	NM	130	LiF	267	323	0.931	17.2	991	460−570
E5 (95-033)	NM + EDA	2	LiF	264	ambient	0.902	16.6	927	390−610
E6 (96-017)	NM + EDA	105	sapphire	290	ambient	0.535	12.1	734	380−750
E7 (95-018)	NM + EDA	3	sapphire	262	ambient	0.605	13.7	762	460−570
E8 (95-019)	NM + EDA	50	sapphire	249	ambient	0.621	14.1	769	460−570
E9 (95-011)	NM + EDA	135	sapphire	269	ambient	0.612	13.9	765	460−570
A4 (95-028)[b]	NM + EDA	0	sapphire	257	ambient	0.543	12.2	737	420−650

[a] Typical ring-up times to reach 95% of the peak pressure are 130 and 300 ns with LiF and sapphire front windows, respectively. [b] Absorption experiment of ref 3.

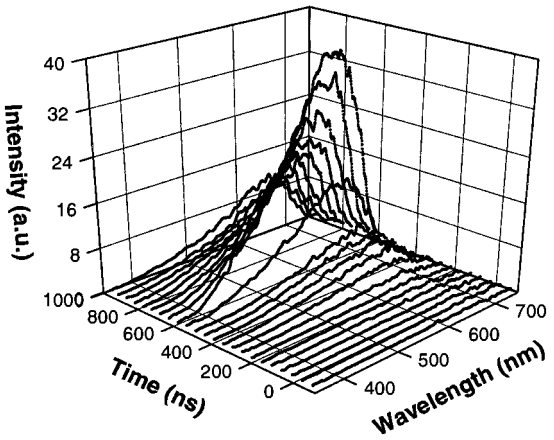

Figure 2. Time-resolved emission spectra of neat NM shocked to 16.7 GPa (experiment E2). At 0 ns shock enters the sample; by 120 ns, the final pressure is reached. The sample was heated to 50 °C before the experiment. Spectra were taken with 48 ns resolution.

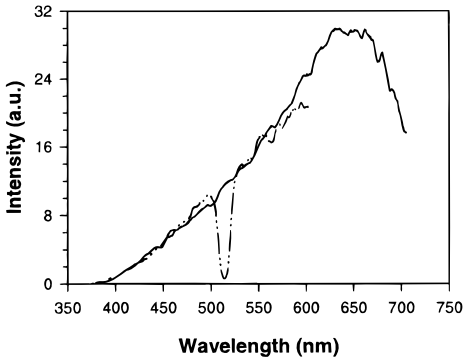

Figure 3. Emission spectra of neat NM measured at 600 ns (solid line, experiment E2) and a NM−EDA mixture measured at 370 ns (dashed−dotted line, experiment E5). Time is relative to the instant when the shock wave entered the sample. The dip at 514 nm corresponds to the holographic notch filter in experiment E5; no filter was present in the optical path in experiment E2. Spectral coverage in experiment E5 was narrower than in experiment E2.

the experiment, i.e., the "blue" threshold at 390 nm and the maximum around 650 nm.

Thermal radiation due to heat generated by the reaction cannot explain the observed emission because the peak at 650 nm would correspond to a temperature of about 4500 K. Such a temperature due to reaction onset is not reasonable since the thermodynamic temperature even in a fully developed detonation is about 3900 K.[18] Moreover, the gray-body emission spectrum at any temperature does not match the observed spectrum. Hence, luminescence from reaction products seems to be a more plausible explanation. In fact, the abundance of internal energy

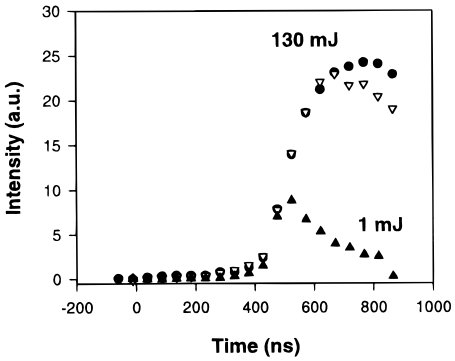

Figure 4. Kinetics of emission for two different laser intensities from neat NM shocked to 17 GPa: (solid triangles) at 494 nm (experiment E3); (dots) at 494 nm (experiment E4); (open triangles at 561 nm (experiment E4). For comparison the intensity at 561 nm is multiplied by 0.6. At 0 ns shock enters the sample. The energy of the laser pulse is shown.

in an energetic material like NM may cause its nascent fragments to form in an electronically excited state. Chemiluminescent phenomena are often observed during shock initiation of energetic materials.[23−25] Time correlation of the emission with other features of reaction observed in Raman and UV−vis absorption experiments[2−9] supports this explanation. Spectrally resolved emission records may suggest the identity of the emitting species. The above-mentioned features of the spectra agree well with the following interpretation:

$$NO_2^* \rightarrow NO_2 + h\nu \qquad (1)$$

Further discussion of this assignment is given in section IV.

Since laser light is used as a probe in numerous experimental methods, it is critical to know how strongly the excitation perturbs the reacting system. In particular, determining the feasibility of Raman measurements in reacting shocked explosives may be of considerable interest.[1] While Raman spectroscopy has proven to be useful for probing the initial stages of chemical reaction in shocked NM,[6] it was not clear if it could be used to probe farther into the reaction sequence. Therefore, we examined the effects of laser excitation in shocked NM using emission spectra as a probe.

In experiments E3 and E4 we used identical configurations except for the laser intensity (see Table 1). The results of these experiments are shown in Figure 4. As can be seen, the kinetics of emission coincide until ca. 500 ns, displaying the same induction period and similar takeoff. However, after 500 ns they diverge. Emission without the laser is quenched, while it keeps growing with the laser. The spectral shape is also slightly different in the two cases. As evident from the kinetics at two

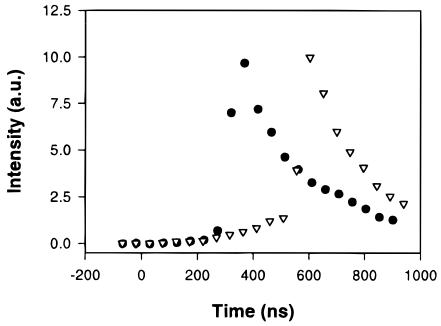

Figure 5. Kinetics of emission at 494 nm: (dots) NM−EDA mixture shocked to 16.6 GPa (experiment E5); (triangles) neat NM shocked to 16.7 GPa (experiment E2). At 0 ns shock enters the sample.

different wavelengths, 494 and 561 nm, the shorter wavelengths part of the spectrum becomes relatively more intense after 700 ns in experiment E4. Thus, laser excitation makes a significant difference in the emission spectra after 500 ns. On the other hand, the initiation stage seems unaffected. The discussion of these results is postponed to section IV.

B. Nitromethane−Ethylenediamine Mixture. In experiment E5 we examined emission from the shocked NM−EDA mixture to compare with neat NM data (experiment E2). However, the spectral coverage (390−610 nm) in experiment E5 was narrower than in experiment E2. The results of these two experiments are compared in Figures 3 and 5. As seen in Figure 5, the emission kinetics were qualitatively very similar, although the timing of the flash was different. The flash of emission in the NM−EDA mixture occurred ca. 250 ns earlier than that in neat NM. This is in agreement with the result that amines sensitize NM.[10−14] The emission spectrum obtained is shown in Figure 3. In the region, where the spectra of experiments E2 and E5 overlap, they have nearly identical shapes. Thus, on the basis of similarities in spectral shapes and qualitative kinetics observed for neat NM and the NM−EDA mixture, one can conclude that the same process, namely, chemiluminescence via reaction 1, is likely to be the source of emission in both cases.

As proposed in our previous paper,[3] the decomposition in shocked amine-sensitized NM proceeds via formation of an intermediate identified as the radical anion of NM. The radical anion is expected to fluoresce (see the discussion in section IVB) when excited to the electronic state located about 2.3 eV above the ground state. Therefore, detection of this fluorescence in shocked NM−amine mixtures would support independently the conclusions regarding the intermediate in ref 3. For this purpose we performed experiment E6.

Three representative spectra from experiment E6 are shown in Figure 6. Three components of the spectra were evident: NM Raman modes and two emission components. While Raman modes were easy to locate and subtract, the other two were convoluted. However, by noting that fluorescence must occur at wavelengths longer than the excitation wavelength (514 nm) while emission due to reaction 1 should be spectrally similar to that in experiments E2 and E5, one can decouple the two temporally by plotting emitted light intensity versus time at wavelengths shorter and longer than 514 nm. The kinetics at two wavelengths are shown in Figure 7. Between 300 and 550 ns, the spectra are dominated by the component with features typical of fluorescence. This observation implies fluorescence in experiment E6.

Further characterization of the fluorescing species can be made by comparing experiment E6 with the absorption experiment, A4, of ref 3. As seen in Table 1, the parameters of both

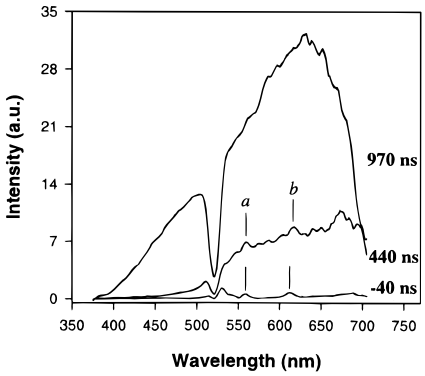

Figure 6. Time-resolved emission spectra of the NM−EDA mixture shocked to 12.1 GPa with 105 mJ/pulse laser intensity (experiment E6). Spectra were taken with 48 ns resolution. At 0 ns shock entered the sample. Only spectra at −40, 440, and 970 ns are shown. Vertical lines mark positions of the Raman modes of NM: (a) convoluted NO_2 stretch/CH_3 bend at ∼1400 cm^{-1} (or 554 nm) and (b) CH_3 stretch at ∼3000 cm^{-1} (or 608 nm). The Raman modes can be noticed as small humps under the vertical lines. The dip at 514 nm corresponds to the holographic notch filter.

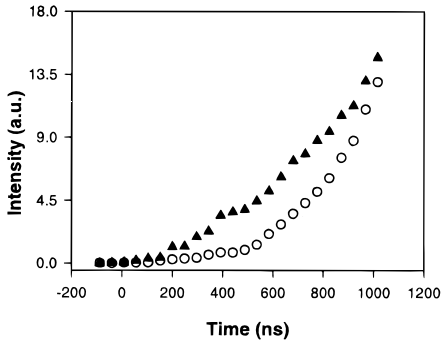

Figure 7. Kinetics of emission of the NM−EDA mixture shocked to 12.1 GPa with 105 mJ/pulse laser intensity (experiment E6): (triangles) at 550 nm; (circles) at 483 nm. For comparison the intensity at 550 nm is multiplied by 0.68. At 0 ns shock enters the sample.

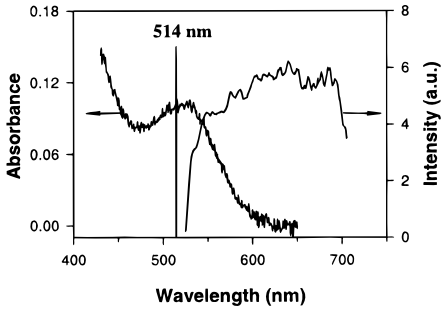

Figure 8. Fluorescence and absorption spectra of the NM−EDA mixture shocked to 12 GPa. The spectra were detected at 440 ns after shock entered the sample in experiments E6 and A4, respectively. The excitation wavelength is shown as a vertical line.

experiments were very similar. An absorption spectrum from experiment A4 along with the fluorescence spectrum from experiment E6 is shown in Figure 8; the intermediate giving rise to the transient absorption peak at ca. 525 nm is likely to cause fluorescence. This conclusion is further supported by a comparison of the kinetics. To obtain the fluorescence kinetics, we assumed the spectral shape of chemiluminescence in experiment E6 to be the same as experiments E2 and E5. We scaled the latter to fit a given spectrum in experiment E6 at wavelengths shorter than 514 nm and then subtracted it. Intensity of the residual at 550 nm is plotted as a function of time in Figure 9 and compared with the absorption peak height.

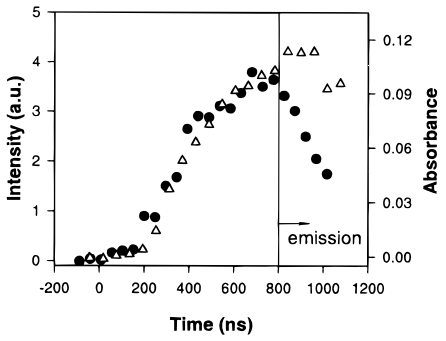

Figure 9. Kinetics of fluorescence at 550 nm (circles) detected in experiment E6 and time evolution of the absorption peak height at 525 nm (triangles) detected in experiment A4. After 800 ns, strong emission in experiment E6 hampers the accurate fluorescence intensity measurements.

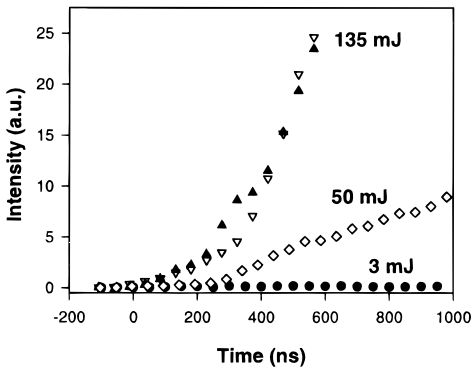

Figure 10. Kinetics of emission of NM−EDA mixtures shocked to 14 GPa: (solid triangles) at 550 nm (experiment E9); (open triangles) at 483 nm (experiment E9); (diamonds) at 483 nm (experiment E8); (dots) at 483 nm (experiment E7). For comparison the intensity at 550 nm is multiplied by 0.68. Fluorescence is evident between 200 and 400 ns as a hump in the kinetics at 550 nm. At 0 ns shock enters the sample. The energy of the laser pulse is shown.

The two coincide until ca. 800 ns which makes a strong case for assigning both to the same species. Discrepancy in the kinetics after 800 ns is ascribed to the fact that the subtraction procedure employed for obtaining the kinetics tends to underestimate the intensity of fluorescence at late times.

Previously, Raman measurements (using excitation at 514 nm) were attempted in shocked sensitized NM.[9] However, the results presented above show that 514 nm excitation light is not appropriate for Raman measurements in sensitized NM. Not only does it introduce a substantial spectral background but it also perturbs the reaction. The latter was demonstrated in experiments E7−E9. Similar to neat NM, we used different laser intensities while monitoring the intensity of light emission from the shocked sample.

Figure 10 shows the significant change in the kinetics of emission in these three experiments at 14 GPa. Turning on the laser changes emission intensity from virtually nothing (experiment E7) to the saturation of the detection system by 600 ns (experiment E9); for the intermediate laser power, the observed emission is of intermediate intensity (experiment E8). These results are discussed in section IVC.

IV. Discussion

A. Chemiluminescence. We base our analysis of chemiluminescence on its general definition as "the emission of light as a result of the generation of electronically excited states formed as a result of a chemical reaction".[26] Therefore, no laser excitation is necessary for chemiluminescence to occur, although it can be influenced by the laser excitation. Here, we limit ourselves to experiments with no (or negligibly low) laser intensity, i.e., experiments E2, E3, and E5. We postpone the discussion of laser effects to section IVC.

As indicated in section IIIA, the observed emission could not be explained as a thermal emission and the most plausible explanation of emission was chemiluminescence. Moreover, reaction 1 seemed to satisfactorily match the characteristics of the detected emission. To demonstrate this, we consider the electronic structure of nitrogen dioxide. The complexity of the NO_2 visible system is due to the fact that in the visible region there are four electronic states each of which can interact with the others.[27] The minima of the $^2B_2$, $^2B_1$, and $^2A_2$ excited states have all been found to be within 2 eV of the minimum of the $^2A_1$ ground state.[28] One of these, the $^2A_2$ state, is not electric dipole connected to the ground state.[28,29] Therefore, emission/absorption in the visible region must be dominated by the other two excited states. The closeness of these states causes mixing of the vibrational levels by vibronic coupling, Jahn− and Renner−Teller, and spin−orbit interactions.[27−29] The equilibrium geometries of both the $^2B_2$ and $^2B_1$ electronic states are substantially different from that of the $^2A_1$ ground state with the ONO angle being 102, 180, and 134°, respectively.[28] Consequently, the Franck−Condon factors between the ground and excited states will be dependent strongly on the wavelength of excitation/emission.

One generates emission spectra of nitrogen dioxide by creating the molecule in the electronic excited state and recording the luminescence upon transition to the ground state. Thus, the details of the spectrum obtained will depend on the vibrational population of the excited state. The emission from the excited states of nitrogen dioxide was observed in a number of processes, e.g. the air afterglow reaction;[30,31] the photodissociation of N_2O_4,[32] nitroalkanes,[33] and nitromethane;[34] the fluorescence,[35−38] etc. When nitrogen dioxide is directly excited by a single wavelength, a discrete structure superimposed on a broad continuum is observed. The sharp lines in the spectra were explained as emission from levels initially populated, whereas the continuum is due to relaxation to a large number of other radiating levels.[39,40] When NO_2* is formed in the chemical reaction, its emission consists primarily of a broad continuum.[30−34]

The ONO angle in nitromethane is 125°.[41,42] This value is somewhat between of those of the $^2A_1$ ground state and the $^2B_2$ excited state of a nitrogen dioxide molecule. If nitrogen dioxide is formed from a nitromethane molecule by C−N bond scission, it is more likely to be in either the $^2A_1$ or $^2B_2$ state. The $^2B_1$ state would require more energy localized on the nitrogen dioxide fragment than the $^2B_2$ state because of geometrical constraints.[28] In gas-phase NO_2, the $^2B_2$ state has a dissociative limit of 390 nm. As can be seen in Figure 3, it coincides with the cutoff of emission. Emission spectra detected in our experiments are also very similar to those detected from the $^2B_2$ state in other processes.[32,33,43] Altogether, it suggests the NO_2 ($^2B_2$) state is the emitting species.

The presence of emission near the dissociative limit of NO_2 indicates that some of the NO_2 product may have been formed with enough internal energy to unimolecularly dissociate to NO + O. The NO formation at some stage of NM decomposition was inferred by several authors.[44,45] From our data we can conclude that if NO is formed at all, it is formed in the ground state. Otherwise, we would have detected the characteristic emission below 390 nm.[46−48]

By comparing neat and sensitized NM spectra and kinetics, we can draw some conclusions about reaction mechanisms. As shown previously, not only is the sensitivity of NM affected by addition of amines[10−14] but the initiation stage seems to be different as well.[3] This difference can result in completely different reaction pathways in neat and sensitized NM. However, on the basis of similarities in spectral shapes and in chemiluminescence kinetics observed in neat and sensitized NM, we conclude that reaction in the bulk (reaction extent larger than ca. 1%) is likely to proceed along the same pathways in both cases; i.e., the reaction schemes converge at some point even though the initiation stages seem different.

To summarize, we presented plausibility arguments for the chemiluminescence accompanying shock-induced decomposition of bulk NM to originate from the NO_2 $X(^2A_1) \leftarrow A(^2B_2)$ transition and inferred the formation of nitrogen dioxide for both neat and sensitized nitromethane. However, on the basis of our data alone, it is difficult to favor any particular mechanism that leads to nitrogen dioxide.

B. Fluorescence. As mentioned earlier, fluorescence was observed only for sensitized NM. The amine can be ruled out as the fluorescing species for the following reason. The 514 nm excitation does not cause the fluorescence of the amine at ambient pressure. The amine does not fluoresce at high pressure either, as demonstrated by the data presented in Figure 9. By 300 ns, the sample is in the final shocked state. Had the fluorescence been caused by the amine, it would have reached the maximum by that time and then declined due to the amine consumption. However, this was not observed in our experiments. The fluorescence begins to appear at 200 ns and keeps increasing until ca. 800 ns. Therefore, it can be assigned to an intermediate specific to the reaction pathway in sensitized NM. Also, as indicated in section IIIB, the data strongly suggested the fluorescing species was the same as the species that gave rise to the absorption peak at 525 nm. Previously, on the basis of our absorption data,[3] we have proposed the latter to be the radical anion of NM: $CH_3NO_2^{\bullet -}$. Next we analyze the electronic structure of the radical anion to assess this assignment.

Unfortunately, very limited data are available on the electronic structure of the radical anion. The ground state is relatively better studied. The information about it was obtained mostly from quantum chemical calculations and ESR spectroscopy.[42,49−51] The electronic excited states were probed indirectly by reactive collisions between neutral NM molecules and alkali atoms.[52,53] Electron promotion to the electronic states of the radical anion produced ionic intermediates for nitromethane fragmentation. Hence, information about the excited states was deduced from energy distributions of the products. This procedure did not provide accurate energies for the electronic transitions but resulted in the potential energy (Morse) curves for the C−N internuclear distance.[52]

The $^1A_1$ ground state of a neutral molecule has a vertical electron affinity of -2.16 ± 0.7 eV, an adiabatic electron affinity of 0.26 ± 0.08 eV and a well depth of 2.52 eV.[42,49−53] Because the NM molecule possesses a large dipole moment of 3.46 D, the radical anion has dipole-bound states in addition to the valence-bound states.[50,51] Three electronic, valence-bound states of $CH_3NO_2^{\bullet -}$ have been identified. The $^2A_1$ ground state of the radical anion is much shallower, 0.56 ± 0.1 eV,[50−52] than that of a neutral molecule. The equilibrium C−N distance for this state is 2.0 Å, which is longer than in a neutral molecule (1.475 Å).[42,52] Experiment and theory predict that in equilibrium the plane containing the two oxygen atoms is tilted with respect to the C−N direction.[49−53]

The two $^2B_1$ excited states have been identified. Both of them are formed by electron attachment to the LUMO of NM, π^* antibonding orbital in the nitro group. The lower $^2B_1$ state correlates asymptotically with the $^3B_1$ (triplet) state of NO_2^-. The upper $^2B_1$ state correlates asymptotically with the $^1B_1$ (singlet) state of NO_2^-. Because the π^* orbital is only weakly antibonding, the potential energy well of these states is rather deep, about 1.5 eV.[52] The asymptotes of the $^2B_1$ states lie 2.3 and 3.2 eV above the $^2A_1$ ground state.[54,55]

Absorption spectroscopy and fluorescence probe vertical up and down electronic transitions respectively between ground and excited states. As seen from the spectra presented in Figure 8, these transitions have maxima around 2.36 and 2.0 eV, respectively. These values are consistent with the transition energies expected between the $^2A_1$ ground state and the upper $^2B_1$ excited state of $CH_3NO_2^{\bullet -}$. Indeed, one can estimate the energies of these transitions from the asymptotic energy gap, ΔE_-, and well depths, E_w, of the corresponding potential energy Morse curves as (a) $\Delta E_- + E_w(^2A_1) - E_w(^2B_1) + \delta(^2B_1)$ for the up transition and (b) $\Delta E_- + E_w(^2A_1) - E_w(^2B_1) - \delta(^2A_1)$ for the down transition. Here δ is the energy change on a corresponding potential energy curve when the C−N distance is changed from the equilibrium value to a distance corresponding to a given vertical transition. Since the C−N equilibrium distances of the $^2A_1$ and $^2B_1$ states are only slightly different (probably ca. 0.3 Å), the δ values are expected to be on the order of several tenths of electronvolt. This puts the transitions in the vicinity of 2.3 eV ($\approx 3.2 + 0.56 - 1.5$) for the upper $^2B_1$ state.

Because of symmetry, the lower $^2B_1$ state is not coupled (electric dipole interaction) to the ground state; the transitions between these two states are restricted. The sensitivity of our detection systems in both absorption and emission experiments did not allow us to observe very weak transitions. Hence, transitions between the ground state and the lower $^2B_1$ state were not observed. On the other hand, dipole allowed excitation to the upper $^2B_1$ state should lead to fluorescence because (a) the fairly deep potential energy well stabilizes it against dissociation; (b) the π character of the orbital stabilizes it against autodetachment by the centrifugal barrier; and (c) there is no ladder of vibrationally excited $^2A_1$ states for effective radiationless relaxations. All of the above considerations make the upper $^2B_1$ state of $CH_3NO_2^{\bullet -}$ a very plausible fluorescing species.

To summarize, our conjecture of the radical anion of NM as a possible fluorescing species, on the basis of its electronic structure, is consistent with our measurements from both absorption[3] and emission experiments. Therefore, the radical anion of NM is inferred as an intermediate in the decomposition process in amine-sensitized NM.

C. Interactions of the Reacting Material with Laser Light. Our experimental data show that the laser excitation at 514 nm affects the reaction in both neat NM and the NM−EDA mixture. The effect is observed essentially as a brighter light emission in both cases. However, it is qualitatively different in the two cases. The initial stage of the reaction seems unaffected by the laser intensity in neat NM in contrast to the NM−EDA mixture. Therefore, we discuss them separately.

Neat Nitromethane. In neat NM, as detected by emission, the laser excitation affects the system well after the initiation stage (induction period in both emission and absorption experiments). By the time this effect becomes apparent (ca. 600 ns), a significant amount of products has been formed as inferred from the absorption data.[3,5] The laser is likely to interact with the products since they absorb light while the unreacted material

does not. After analyzing several possible scenarios, we favor the laser heating mechanism. Given the optical density of the reacting sample, heat capacity, and the laser intensity, we estimated the heating rate in the laser spot to be on the order of 1 K/ns.[56] In a short time, a hot spot will be formed in the sample and the higher temperature may result in a greater portion of NO_2 molecules formed in the excited state. These would increase the radiance via reaction 1 accordingly.

NM−EDA Mixtures. In the case of NM−EDA mixtures, the effect of the laser is qualitatively different, suggesting a different interaction mechanism. For the laser heating to play a role, the absorbance in the sample must exceed 1 at times comparable to the onset of chemiluminescence in experiments E8 and E9, which is around 300 ns or less (see Figure 10). However, as shown previously,[3] at 14 GPa the absorbance at 514 nm did not exceed 0.3 by 650 ns and barely reached 0.9 by 1 μs. Although some laser heating is expected, accounting for the effect observed experimentally would require the activation energy of the rate limiting step to be unrealistically high. Therefore, it is unlikely that laser heating plays a major role here, and we speculate on the possible photochemical mechanism for chemiluminescence enhancement. Among the species that can absorb light at 514 nm there are radical anions,[3] "F" species (see ref 3 for details), and charge-transfer complexes.[13,14] The estimated partition of absorbed light is ~70% by radical anions, ~30% by F species, and ~1% by charge-transfer complexes. Consequently these species might be involved in photochemical processes.

As discussed in the preceding section, the excited states of the radical anion are not dissociative. Therefore, the excitation should not lead to radical anion depletion. The experimental data in Figure 9 seem to indicate the same. Because of no difference in the radical anion kinetics without the laser (experiment A4) and with 105 mJ/pulse laser excitation (experiment E6), it is reasonable to conclude that this particular intermediate is not susceptible to photolysis by the 514 nm light.

Unfortunately, the identity of F species is unknown owing to the lack of understanding of the reaction mechanism.[3] Therefore, it is difficult to evaluate its susceptibility to photolysis. Regarding charge-transfer complexes, we have examined their decomposition by the 514 nm light at ambient pressure. Although in the case of primary amines the charge-transfer band is located around 430 nm, it is quite broad and its tail extends up to 530 nm.[14] When the NM−EDA mixture was irradiated with 514 nm light at ambient conditions, the charge-transfer band slowly diminished, indicating that photochemical processes did take place. Under high pressure the light absorption by charge-transfer complexes will likely be enhanced due to band-broadening and red-shifting.[57] Higher temperature may also enhance the reaction rate. Thus, photochemical decomposition of charge-transfer complexes may play a role even though they absorb a small fraction of light.

A plausible reaction scheme that takes into account all of the above considerations and illustrates our observations and conjectures is shown in Figure 11. With no light present the decomposition mechanism in NM−EDA mixtures can be described as follows. During the initiation stage (I), the NM−amine interaction results in the formation of several intermediates, one of which has been shown to be $CH_3NO_2^{\bullet-}$. These intermediates further react (stage II) to produce radical and ion species that are able to sustain chain reactions (III) in the bulk of NM. The latter eventually leads to an explosion/detonation and the final products, stage IV. Stage IV is not observable on our time scale. Methyl radicals and nitrogen dioxide are

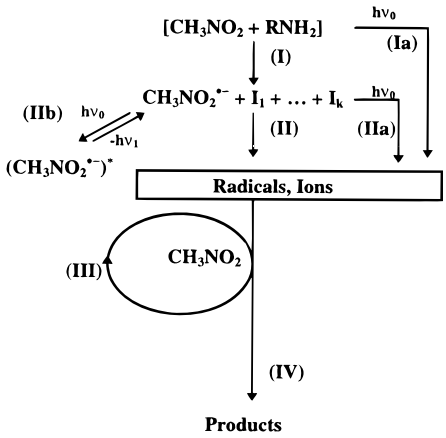

Figure 11. Block diagram of proposed reaction flow in shocked NM−EDA mixtures. $h\nu_0 = 2.41$ eV; $\nu_1 < \nu_0$. More detailed description is given in the text.

believed to play an important role in stage III.[13,14] Some of the nitrogen dioxide molecules are formed in the excited state, resulting in chemiluminescence via reaction 1 as discussed in section IVA. Under intense laser irradiation the initial supply of radicals and/or ions for stage III is enhanced by photochemical reactions Ia and/or IIa. This could trigger formation of NO_2* within stage III more effectively, and, therefore, one would see brighter chemiluminescence via reaction 1. Fluorescence can also be observed as represented by reaction IIb.

Although the scheme in Figure 11 accounts quite well for the experimental observations, we attempted to further evaluate the feasibility of this scheme and the relative importance of reactions Ia and IIa by kinetic modeling. Stage III was modeled by the cubic autocatalytic process,[13,14] while intensity of chemiluminescence was assumed to be proportional to the overall reaction rate. The modeling showed that the scheme was able to predict well the observed difference in chemiluminescence intensity (Figure 10) with a single parameter—light intensity. However, either of the reactions Ia or IIa, when included in the scheme, gave essentially the same result. We, therefore, could not conclusively prefer one over the other.

It is important to recognize that the intensity of chemiluminescence may or may not be interpreted as a measure of global reaction rate and/or extent. Since chemiluminescence originates specifically in reaction 1, it may be reliably interpreted as a measure of that particular reaction rate only. Since there are no direct data on the relative weight of NO_2* formation in stage III, it is quite possible that it does not reflect well the kinetics of the entire process. From our data we can definitely conclude that the rate of reaction 1 is indeed affected significantly by the laser, but it is not very straightforward to extrapolate this statement further.

V. Summary

We have presented results of an emission study of shock-induced chemical reactions in neat and amine-sensitized NM. The results are summarized as follows.

Shock-induced reactions in NM are accompanied by light emission. Broadband emission identified as chemiluminescence was observed for both neat and sensitized NM. Chemiluminescence spectra suggest the formation of NO_2 in shocked reacting NM. A fraction of it is formed in an electronically excited state, giving rise to chemiluminescence.

When laser light at 514 nm is present, fluorescence in addition to the chemiluminescence is observed in shocked NM−EDA mixtures. No such fluorescence is found in neat NM. The

fluorescing species has been assigned to an intermediate formed in the first step of shock-induced decomposition in NM−EDA mixtures. The same intermediate was also detected with transient absorption spectroscopy,[3] and it was inferred to be the radical anion of NM: $CH_3NO_2^{\bullet-}$. On the basis of the analysis of the electronic structure of $CH_3NO_2^{\bullet-}$, we found this interpretation to be consistent with the fluorescence data.

Intense laser irradiation (~10 MW/cm^2 at 514 nm) results in significantly brighter chemiluminescence in both neat NM and NM−EDA mixtures. However, this effect is qualitatively different in the two cases. In neat NM, the onset of chemiluminescence does not depend on the laser power. In contrast, the onset of chemiluminescence in NM−EDA mixtures shifts strongly to earlier times as the laser power increases. We attributed this difference to different mechanisms operative initially in neat and sensitized NM. Several possible scenarios of light interaction with the shocked material were considered.

Acknowledgment. D. Savage and K. Zimmerman are thanked for their assistance in the experimental effort. Discussions with Dr. J. M. Winey and Dr. G. I. Pangilinan are gratefully acknowledged. This work was supported by ONR Grant N00014-93-1-0369 (Program Manager: Dr. R. S. Miller).

References and Notes

(1) Gupta, Y. M. *J. Phys. IV, Colloque C4*, **1995**, *5*, C4−345.
(2) Constantinou, C. P.; Winey, J. M.; Gupta, Y. M. *J. Phys. Chem.* **1994**, *98*, 7767.
(3) Gruzdkov, Y. A.; Gupta, Y. M. *J. Phys. Chem. A* **1998**, *102*, 2322.
(4) Winey, J. M. *Time-resolved optical spectroscopy to examine shock-induced decomposition in liquid nitromethane.* Ph.D. Dissertation, Washington State University, 1995.
(5) Winey, J. M.; Gupta, Y. M. *J. Phys. Chem. A* **1997**, *101*, 9333.
(6) Winey, J. M.; Gupta, Y. M. *J. Phys. Chem. B* **1997**, *101*, 10733.
(7) Winey, J. M.; Knudson, M. D.; Duvall, G. E.; Gupta, Y. M. Manuscript in preparation.
(8) Pangilinan, G. I.; Gupta, Y. M. *J. Phys. Chem.* **1994**, *98*, 4522.
(9) (a) Gupta, Y. M.; Pangilinan, G. I.; Winey, J. M.; Constantinou, C. P. *Chem. Phys. Lett.* **1995**, *232*, 341. The conclusions drawn in this paper are no longer believed to be valid, as discussed in: (b) Gupta, Y. M.; Gruzdkov, Y. A.; Pangilinan, G. I. *Chem. Phys. Lett.* **1998**, *283*, 251.
(10) Engelke, R. *Phys. Fluids* **1980**, *23*, 875.
(11) Engelke, R.; Earl, W. L.; Rohlfing, C. M. *J. Chem. Phys.* **1986**, *84*, 142.
(12) Cook, M. D.; Haskins, P. J. In *Proceedings of the 19th International Annual Conference of ICT on Combustion and Detonation Phenomena*, Karlsruhe, Germany; Fraunhofer Institut fur Chemische, Technologie, Explosivstoffe: Karlsruhe, Germany, 1988; p 85−1.
(13) Costantinou, C. P.; Mukundan, T.; Chaudhri, M. M. *Philos. Trans. R. Soc. London A* **1992**, *339*, 403.
(14) Constantinou, C. P. *The nitromethane-amine interaction.* Ph.D. Dissertation, Cambridge University, Cambridge, U.K., 1992.
(15) Blais, N. C.; Engelke, R.; Sheffield, S. A. *J. Phys. Chem. A* **1997**, *101*, 8285.
(16) Piermarini, G. J.; Block, S.; Miller P. J. *J. Phys. Chem.* **1989**, *93*, 457.
(17) Hardesty, D. R. *Combust. Flame* **1976**, *27*, 229.
(18) Yoo, C. S.; Holmes, N. C. *High Pressure Science and Technology, Conference Proceedings*, Colorado Springs, CO; American Institute of Physics: New York, 1993; Part 2, p 1567.
(19) Fowles, G. R.; Duvall, G. E.; Asay, J.; Bellamy, P.; Feistman, F.; Grady, D.; Michaels, T.; Mitchell, R. *Rev. Sci. Instrum.* **1970**, *41*, 984.
(20) Ogilvie, K. M.; Duvall, G. E.; Collins, R. *SHOCKUP Computer Code*; Shock Dynamics Center, Washington State University: Pullman, WA, 1984.
(21) Barker, L. M.; Hollenbach, R. E. *J. Appl. Phys.* **1970**, *41*, 4208.
(22) Carter, W. J. *High Temperatures−High Pressures* **1973**, *5*, 313.
(23) Dick, J. J.; Mulford, R. N.; Spencer, W. J.; Pettit, D. R.; Garcia, E.; Shaw, D. C. *J. Appl. Phys.* **1991**, *70*, 3572.
(24) Dick, J. J. *J. Phys. IV*, Colloque C4 **1995**, *5*, C4−103.
(25) Trott, W. M.; Renlund, A. M. *Proc. 8th Symp. (Int.) Detonation* **1985**, 691.
(26) Gundermann, K. D.; McCapra, F. *Chemiluminescence in Organic Chemistry*; Springer-Verlag: Berlin, 1987; p 7.
(27) Hsu, D. K.; Monts, D. L.; Zare, R. N. *Spectral Atlas of Nitrogen Dioxide 5530 to 6480 Å*; Academic Press: New York, 1978.
(28) Gillespie, G. D.; Khan, A. U.; Wahl, A. C.; Hosteny, R. P.; Krauss, M. *J. Chem. Phys.* **1975**, *63*, 3425.
(29) Gillespie, G. D.; Khan, A. U. *J. Chem. Phys.* **1976**, *65*, 1624.
(30) Kaufman, F. In *Chemiluminescence and Bioluminescence*; Cormier, M. J., Hercules, D. M., Lee, J., Eds.; Plenum Press: London, 1973; p 83.
(31) Gaydon, A. G. *The Spectroscopy of Flames*; Wiley: New York, 1974.
(32) Inoue, G.; Nakata, Y.; Usui, Y.; Akimoto, H.; Okuda, M. *J. Chem. Phys.* **1979**, *70*, 3689.
(33) Butler, L. J.; Krajnovich, D.; Lee, Y. T.; Ondrey, G.; Bersohn, R. *J. Chem. Phys.* **1983**, *79*, 1708.
(34) Haugen, G. R.; Steinmetz, L. L. *Mol. Photochem.* **1979**, *9*, 473.
(35) Abe, K.; Meyers, F.; McCubbin, T. K.; Polo, S. R. *J. Mol. Spectrosc.* **1971**, *38*, 552.
(36) Abe, K. *J. Mol. Spectrosc.* **1973**, *48*, 395.
(37) Stevens, C. G.; Zare, R. N. *J. Mol. Spectrosc.* **1975**, *56*, 167.
(38) Stevens, C. G.; Swagel, M. W.; Wallace, R.; Zare, R. N. *Chem. Phys. Lett.* **1973**, *18*, 465.
(39) Donelly, V. M.; Kauffman, F. *J. Chem. Phys.* **1978**, *69*, 1456.
(40) Keil, D. G.; Donelly, V. M.; Kauffman, F. *J. Chem. Phys.* **1980**, *73*, 1514.
(41) Cox, A. P.; Waring, S. *J. Chem. Soc., Faraday Trans. 2*. **1972**, *68*, 1060.
(42) Ramondo, F. *Can. J. Chem.* **1992**, *70*, 314.
(43) Okabe, H. *Photochemistry of Small Molecules*; Wiley-Interscience: New York, 1978; p 232.
(44) Guirguis, R.; Hsu, D.; Bogan, D.; Oran, E. *Combust. Flame* **1985**, *61*, 51.
(45) Melius, C. F. *J. Phys. IV*, Colloque C4 **1995**, *5*, C4−535.
(46) Frosch, R. P.; Robinson, G. W. *J. Chem. Phys.* **1964**, *41*, 367.
(47) Irvine, A. M. L.; Smith, I. W. M.; Tuckett, R. P. *J. Chem. Phys.* **1990**, *93*, 3187.
(48) Chen, K.; Pei, C. *Chem. Phys. Lett.* **1987**, *137*, 361.
(49) Gilbert, B. C.; Trenwith, M. *J. Chem. Soc., Perkin Trans. 2* **1973**, *14*, 2010.
(50) Gutsev, G. L.; Bartlett, R. J. *J. Chem. Phys.* **1996**, *105*, 8785.
(51) Compton, R. N.; Carman, H. S.; Desfrancois, C.; Abdoul-Carmine, H.; Schermann, J. P.; Hendricks, J. H.; Lyapustina, S. A.; Bowen, K. H. *J. Chem. Phys.* **1996**, *105*, 3472.
(52) Lobo, R. F. M.; Moutinho, A. M. C.; Lacmann, K.; Los, J. *J. Chem. Phys.* **1991**, *95*, 166.
(53) Compton, R. N.; Reinhardt, P. W.; Cooper, C. D. *J. Chem. Phys.* **1978**, *68*, 4360.
(54) Kimura, M.; Lacmann, K. *Chem. Phys. Lett.* **1980**, *70*, 41.
(55) Trawick, W. G.; Eberhardt, W. H. *J. Chem. Phys.* **1954**, *22*, 1462.
(56) Estimates of the heating rate, R, were made as follows: $R = I/(C\rho d)$ where I is the intensity of the laser light, C is the specific heat, ρ is the density, and d is the thickness of the light absorbing layer. Using an I value of ~10 MW/cm^2, handbook values for the specific heat and density of ~1 J/(g K) and ~1 g/cm^3, respectively, and a d value of 100 μm, we have estimated R to be ca. 1 K/ns.
(57) Drickamer, H. G.; Frank, C. W. *Electronic Transitions and the High Pressure Chemistry and Physics of Solids;* Chapman and Hall: London, 1973; p 98.